Pergamon

Int. J. Heat Mass Transfer. Vol. 37, No. 17, pp. 2699–2706, 1994

0017-9310/94 $7.00+0.00

0017-9310(94)E0096-D

Transient heat transfer in simultaneously developing channel flow with step change in inlet temperature

R. O. C. GUEDES and M. N. OZISIK†

Mechanical Aerospace Engineering Department, North Carolina State University, Raleigh, NC 27695-7910, U.S.A.

(*Received* 27 *October* 1993 *and in final form* 28 *February* 1994)

Abstract—The transient heat transfer in forced convection for simultaneously developing laminar flow inside a parallel-plate channel is studied by solving the steady momentum equation with the generalized integral transform technique and the transient energy equation through a hybrid approach that combines the integral transform method with a second-order accurate finite-differences scheme. Semi-analytical results are then presented for the fluid bulk temperature and local Nusselt number along the channel as a function of position and time.

1. INTRODUCTION

HEAT transfer is hydrodynamically and thermally developing forced convection inside ducts is of great interest in heat-exchanger design, as documented in the vast literature survey compiled by Shah and London [1] and Shah and Bhatti [2].

In the earlier solution of such problems [3–5], the linearization procedure developed by Langhaar [6] and Sparrow *et al.* [7] was used in order to obtain approximate but explicit expressions for the velocity components. The energy equation was then numerically solved for the temperature distribution with finite-differences, after neglecting the radial convection term.

Recently, a similar approach has been followed [8], but the energy equation was solved with the generalized integral transform technique, and the influence of the radial convection was investigated.

Carvalho *et al.* [9] solved the entrance region velocity problem with the generalized integral transform technique by making a boundary layer approximation for the flow field. Cotta [10] solved the entrance-region heat transfer problem with the generalized integral transform technique by using the velocity profile developed in ref. [9].

Other simultaneously developing steady-state solutions of thermal entrance problems include the use of finite-differences [11–13], the integral method [14] and an approximate analytical solution [15].

All of the aforementioned works deal with the steady situation. For transient forced convection in ducts, several investigations have been conducted [16–20] for hydrodynamically developed but thermally developing flow while, in the case of simultaneously developing transient forced convection, the literature is scarce. Recently, Schutte *et al.* [17] investigated numerically the transients resulting from a step change in the wall heat flux. To the knowledge of the authors, no solution appears to be available for the simultaneously developing transient thermal entry problem resulting from a variation of the duct inlet temperature.

In this work, we intend to fill this gap in the literature by presenting a solution for the case of simultaneously developing transient forced convection resulting from a step change in inlet temperature.

2. MATHEMATICAL FORMULATION

We consider a developing, steady-state, laminar flow of a Newtonian fluid inside a parallel-plate duct. The static pressure is assumed uniform across the cross section, and the axial shear component is negligible relative to the transverse shear component. At time $t = 0$, the inlet temperature undergoes a step change, while a constant temperature is maintained at the duct wall. The continuity and momentum equations of developing steady flow are given in the dimensionless form as

$$\frac{\partial U(R,Z)}{\partial Z}+\frac{\partial V(R,Z)}{\partial R}=0 \quad 0<R<1, Z>0 \tag{1a}$$

$$U(R,Z)\frac{\partial U(R,Z)}{\partial Z}+V(R,Z)\frac{\partial U(R,Z)}{\partial R}$$

$$=-\frac{\mathrm{d}P^*}{\mathrm{d}Z}+\frac{1}{Re}\frac{\partial^2 U(R,Z)}{\partial R^2} \quad 0<R<1, Z>0. \tag{1b}$$

† Author to whom correspondence should be addressed.

NOMENCLATURE

D_h	hydraulic diameter of parallel-plate
M_i	norm of problem (18)
N_i	norm of problem (10)
N	truncation order
$Nu(Z)$	local Nusselt number
P, P^*	static pressure (dimensional and dimensionless)
Pr	Prandtl number
Pe	Peclet number
Re	Reynolds number
r, R	normal coordinate (dimensional and dimensionless)
r_w	half the spacing between parallel plates
$T(r,z)$	temperature distribution (dimensional)
T_0	uniform inlet temperature
T_w	prescribed wall temperature
$u(r,z), U(R,Z)$	axial velocity components (dimensional and dimensionless)
u_0	inlet flow velocity
$v(r,z), V(R,Z)$	normal velocity components (dimensional and dimensionless)
z, Z	axial coordinates (dimensional and dimensionless).

Greek symbols

α	thermal diffusivity of fluid
$\Theta(R,Z)$	dimensionless temperature distribution
λ_i	eigenvalues of problem (18)
μ_i	eigenvalues of problem (10)
ν	kinematic viscosity
τ	dimensionless time.

The transient energy equation, assuming constant physical properties and neglecting viscous dissipation, axial conduction and free convection, is taken as

$$\frac{\partial\Theta(R,Z,\tau)}{\partial\tau}+Pe\left(U(R,Z)\frac{\partial\Theta(R,Z,\tau)}{\partial Z}+V(R,Z)\frac{\partial\Theta(R,Z,\tau)}{\partial R}\right)=\frac{\partial^2\Theta(R,Z,\tau)}{\partial R^2}$$

$$0<R<1,\ Z>0. \quad (1c)$$

The boundary conditions for the velocity are given by

$$U(R,0)=1 \quad V(R,0)=0$$

$$\frac{\partial U(0,Z)}{\partial R}=0 \quad V(0,Z)=0$$

$$U(1,Z)=0 \quad V(1,Z)=0. \quad (2a\text{–}f)$$

The initial and boundary conditions for the temperature are taken as

$$\Theta(R,Z,\tau)=0 \quad \tau=0$$

$$\Theta(R,0,\tau)=1 \quad \tau>0$$

$$\frac{\partial\Theta(0,Z,\tau)}{\partial R}=0 \quad \tau\geqslant 0$$

$$\Theta(1,Z,\tau)=0 \quad \tau\geqslant 0 \quad (3a\text{–}d)$$

where various dimensionless groups are defined as

$$R=\frac{r}{r_w};\quad Z=\frac{z}{r_w};\quad U=\frac{u}{u_0};\quad V=\frac{v}{u_0};$$

$$P^*=\frac{P}{\rho u_0^2};\quad \tau=\frac{\alpha t}{r_w^2};\quad \Theta=\frac{T-T_w}{T_0-T_w};\quad Re=\frac{u_0 r_w}{\nu};$$

$$Pe=Re\,Pr;\quad Pr=\frac{\nu}{\alpha}. \quad (4)$$

We split up the velocity field in the form

$$U(R,Z)=U^*(R,Z)+U_\infty(R) \quad (5a)$$

where

$$U_\infty(R)=\tfrac{3}{2}(1-R^2). \quad (5b)$$

Introducing the velocity profiles given by equations (5) into the continuity, momentum and energy equations (1a–c), we obtain

$$\frac{\partial U^*(R,Z)}{\partial Z}+\frac{\partial V(R,Z)}{\partial R}=0 \quad (6a)$$

$$[U^*(R,Z)+U_\infty(R)]\frac{\partial U^*(R,Z)}{\partial Z}+V(R,Z)\left(\frac{\partial U^*(R,Z)}{\partial R}-3R\right)=-\left(\frac{dP^*}{dZ}+\frac{3}{Re}\right)+\frac{1}{Re}\frac{\partial^2 U^*(R,Z)}{\partial R^2} \quad (6b)$$

$$\frac{\partial\Theta(R,Z,\tau)}{\partial\tau}+Pe\left((U^*(R,Z)+U_\infty(R))\frac{\partial\Theta(R,Z,\tau)}{\partial Z}+V(R,Z)\frac{\partial\Theta(R,Z,\tau)}{\partial R}\right)=\frac{\partial^2\Theta(R,Z,\tau)}{\partial R^2} \quad (6c)$$

and the inlet and boundary conditions for the velocity field become

$$U^*(R,0)=1-U_\infty(R) \quad (7a)$$

$$\frac{\partial U^*(0,Z)}{\partial R}=0 \quad (7b)$$

$$U^*(1, Z) = 0 \tag{7c}$$

while the initial and boundary conditions for the temperature field remain unaltered.

The purpose of such a splitting-up is to enhance the computational performance in the solution of the velocity field.

3. SOLUTION FOR THE VELOCITY FIELD

The momentum and continuity equations being uncoupled from the energy equation, the velocity field can be solved separately from the temperature problem as described below.

First, the continuity equation (6a) is integrated over the duct cross section to give

$$V(R, Z) = \int_R^1 \frac{\partial U^*(R', Z)}{\partial Z} \, dR'. \tag{8}$$

Similarly, the momentum equation (6b) is integrated over the duct cross section to yield an expression for the pressure gradient as

$$-\frac{dP^*}{dZ} = 2\int_0^1 (U^*(R, Z) + U_\infty(R)) \frac{\partial U^*(R, Z)}{\partial Z} \, dR - \frac{1}{Re}\frac{\partial U^*(1, Z)}{\partial R} + \frac{3}{Re}. \tag{9}$$

We now consider the following auxiliary eigenvalue problem:

$$\frac{d^2\psi(\mu_i, R)}{dR^2} + \mu_i^2 \psi(\mu_i, R) = 0 \quad 0 < R < 1 \tag{10a}$$

$$\frac{d\psi(\mu_i, 0)}{dR} = 0 \tag{10b}$$

$$\psi(\mu_i, 1) = 0 \tag{10c}$$

whose eigenvalues, eigenfunctions and the normalization integral are given, respectively, by

$$\mu_i = (2i-1)\pi/2 \tag{11a}$$

$$\psi(\mu_i, R) = \cos \mu_i R \tag{11b}$$

$$N_i = \int_0^1 \psi^2(\mu_i, R) \, dR = 1/2. \tag{11c}$$

An integral transform pair is constructed by utilizing the eigenvalue problem (10):

$$U^*(R, Z) = \sum_{i=1}^{\infty} \frac{\psi(\mu_i, R)}{N_i^{1/2}} \bar{U}_i^*(Z) \quad \text{inversion} \tag{12a}$$

$$\bar{U}_i^*(Z) = \int_0^1 \frac{\psi(\mu_i, R)}{N_i^{1/2}} U^*(R, Z) \, dR \quad \text{transform}. \tag{12b}$$

By introducing $U^*(R, Z)$, as defined by equation (12a), into equations (8) and (9), we obtain expressions for $V(R, Z)$ and dP^*/dZ in terms of the transform $\bar{U}_i^*(Z)$:

$$V(R, Z) = \sum_{j=1}^{\infty} F_j(R) \frac{d\bar{U}_j^*(Z)}{dZ} \tag{13}$$

$$-\frac{dP^*}{dZ} = 2\sum_{j=1}^{\infty} \bar{U}_j^*(Z) \frac{d\bar{U}_j^*(Z)}{dZ} - \frac{1}{Re}\sum_{j=1}^{\infty} \frac{d\psi(\mu_j, 1)}{dR} \frac{\bar{U}_j^*(Z)}{N_j^{1/2}} + \sum_{j=1}^{\infty} H_j^* \frac{d\bar{U}_j^*(Z)}{dZ} + \frac{3}{Re} \tag{14}$$

where

$$F_j(R) = \frac{1}{N_j^{1/2}} \int_R^1 \psi(\mu_j, R') \, dR' \tag{15a}$$

$$H_j^* = \frac{1}{N_j^{1/2}} \int_0^1 U_\infty(R)\psi(\mu_j, R) \, dR - 3\int_0^1 RF_j(R) \, dR. \tag{15b}$$

Next, we take the integral transform of the momentum equation (6b), namely, we operate on equation (6b) with the operator

$$\int_0^1 \psi(\mu_i, R)/N_i^{1/2} \, dR.$$

Then, in the resulting expression, we replace $U^*(R, Z)$, $V(R, Z)$ and P^* by their equivalent formulas (12a), (13) and (14), respectively, to yield

$$\sum_{k=1}^{\infty}\sum_{j=1}^{\infty} [(A_{ijk} + B_{ijk} - 2F_i(0)\delta_{jk})\bar{U}_j^*(Z) + \delta_{jk}(C_{ik} - F_i(0)H_k^*)] \frac{d\bar{U}_k^*(Z)}{dZ} = -\left(\frac{F_i(0)}{N_k^{1/2} Re}\frac{d\psi(\mu_k, 1)}{dR} + \delta_{ik}\frac{\mu_i^2}{Re}\right)\bar{U}_k^*(Z), \quad i = 1, 2, \ldots, \infty \tag{16a}$$

where

$$A_{ijk} = \frac{1}{N_i^{1/2} N_j^{1/2} N_k^{1/2}} \int_0^1 \psi(\mu_i, R)\psi(\mu_j, R)\psi(\mu_k, R) \, dR \tag{16b}$$

$$B_{ijk} = \frac{1}{N_i^{1/2} N_j^{1/2}} \int_0^1 \psi(\mu_i, R) \frac{d\psi(\mu_j, R)}{dR} F_k(R) \, dR \tag{16c}$$

$$C_{ik} = \frac{3}{2N_i^{1/2} N_k^{1/2}} \int_0^1 (1-R^2)\psi(\mu_i, R)\psi(\mu_k, R) \, dR - \frac{3}{N_i^{1/2}} \int_0^1 R\psi(\mu_i, R)F_k(R) \, dR \tag{16d}$$

$$\delta_{ik} = 0, \text{ for } i \neq k \quad \text{or } \delta_{ik} = 1, \text{ for } i = k. \quad (16e)$$

In the above integral transform procedure, the boundary conditions for the velocity problem are already utilized. Finally, when the inlet condition (7a) is transformed, we obtain

$$\bar{U}_i^*(Z) = F_i(0) - E_i \quad \text{at } Z = 0, \quad i = 1, 2, \ldots, \infty \quad (17a)$$

where

$$E_i = \frac{1}{N_i^{1/2}} \int_0^1 U_\infty(R)\psi(\mu_i, R)\,dR. \quad (17b)$$

The system given by equation (16a) provides an infinite set of coupled ordinary differential equations for the transform of velocity $\bar{U}_i^*(Z)$ subjected to the transformed inlet condition (17a). For computational purposes, this system of equations is truncated to a sufficiently large order N, which can be solved by the subroutine DIVPAG from the IMSL package [22].

Once the transformed velocity $\bar{U}_i^*(Z)$ has been numerically computed, the velocity field $U^*(R, Z)$ is recovered by inverting $\bar{U}_i^*(Z)$ according to the inversion formula (12a).

4. SOLUTION FOR THE TEMPERATURE FIELD

Knowing the velocity distribution, we are now in a position to solve the energy equation by following a methodology similar to the one presented previously. We consider an auxiliary eigenvalue problem similar to the one given by equations (10), that is

$$\frac{d^2\Gamma(\lambda_i, R)}{dR^2} + \lambda_i^2\Gamma(\lambda_i, R) = 0 \quad 0 < R < 1 \quad (18a)$$

$$\frac{d\Gamma(\lambda_i, 0)}{dR} = 0 \quad (18b)$$

$$\Gamma(\lambda_i, 1) = 0 \quad (18c)$$

which has eigenvalues, eigenfunctions and the normalization integral given, respectively, as

$$\lambda_i = (2i-1)\pi/2 \quad (19a)$$

$$\Gamma(\lambda_i, R) = \cos \lambda_i R \quad (19b)$$

$$M_i = \int_0^1 \Gamma^2(\lambda_i, R)\,dR = \tfrac{1}{2}. \quad (19c)$$

Based on this eigenvalue problem, we define the following integral transform pair:

$$\Theta(R, Z, \tau) = \sum_{i=1}^{\infty} \frac{\Gamma(\lambda_i, R)}{M_i^{1/2}} \bar{\Theta}_i(Z, \tau) \quad \text{inversion} \quad (20a)$$

$$\bar{\Theta}_i(Z, \tau) = \int_0^1 \frac{\Gamma(\lambda_i, R)}{M_i^{1/2}} \Theta(R, Z, \tau)\,dR \quad \text{transform.} \quad (20b)$$

We now take the integral transform of the energy equation (6c) by the application of the transform (20b). That is, we operate on the energy equation with the operator

$$\int_0^1 \Gamma(\lambda_i, R)/M_i^{1/2}\,dR,$$

to obtain

$$\frac{\partial\bar{\Theta}_i(Z,\tau)}{\partial\tau} + Pe\int_0^1 \frac{\Gamma(\lambda_i, R)}{M_i^{1/2}}(U^*(R,Z) + U_\infty(R))\frac{\partial\Theta(R,Z,\tau)}{\partial Z}\,dR + Pe\int_0^1 \frac{\Gamma(\lambda_i, R)}{M_i^{1/2}} V(R,Z) \times \frac{\partial\Theta(R,Z,\tau)}{\partial R}\,dR = -\lambda_i^2\bar{\Theta}_i(Z,\tau). \quad (21)$$

This equation contains the functions $U^*(R, Z)$ and $\Theta(R, Z, \tau)$ which are now replaced by the equivalent transforms $\bar{U}_i^*(Z)$ and $\bar{\Theta}_i(Z, \tau)$, given by equations (12a) and (20a), respectively, to obtain

$$\frac{\partial\bar{\Theta}_i(Z,\tau)}{\partial\tau} + Pe\sum_{j=1}^{\infty} g_{ij}(Z)\frac{\partial\bar{\Theta}_j(Z,\tau)}{\partial Z} + Pe\sum_{j=1}^{\infty} h_{ij}(Z)\bar{\Theta}_j(Z,\tau) = 0, \quad i = 1, 2, \ldots, \infty \quad (22a)$$

where

$$g_{ij}(Z) = \sum_{k=1}^{\infty} A_{ijk}^*\bar{U}_k^*(Z) + P_{ij}^* \quad (22b)$$

$$h_{ij}(Z) = \sum_{k=1}^{\infty} C_{ijk}^*\frac{d\bar{U}_k^*(Z)}{dZ} + \delta_{ij}\frac{\lambda_i^2}{Pe} \quad (22c)$$

and

$$A_{ijk}^* = \frac{1}{M_i^{1/2}M_j^{1/2}N_k^{1/2}} \times \int_0^1 \Gamma(\lambda_i, R)\Gamma(\lambda_j, R)\psi(\mu_k, R)\,dR \quad (22d)$$

$$P_{ij}^* = \frac{3}{2}\left[\delta_{ij} - \frac{1}{M_i^{1/2}M_j^{1/2}}\int_0^1 R^2\Gamma(\lambda_i, R)\Gamma(\lambda_j, R)\,dR\right] \quad (22e)$$

$$C_{ijk}^* = \frac{1}{M_i^{1/2}M_j^{1/2}}\int_0^1 \Gamma(\lambda_i, R)\Gamma(\lambda_j, R)F_k(R)\,dR. \quad (22f)$$

The system (22) provides an infinite number of coupled first-order partial differential equations for

Table 1. Convergence of the dimensionless axial velocity at the duct centerline for different truncation orders N

X^+	U/U_0 at $R=0$					
	$N=10$	$N=20$	$N=30$	$N=40$	$N=50$	Shah and Bhatti [2]
6.250×10^{-5}	1.0374	1.0480	1.0499	1.0509	1.0514	1.0615
1.250×10^{-4}	1.0637	1.0699	1.0717	1.0725	1.0728	1.0751
2.500×10^{-4}	1.0957	1.1004	1.1016	1.1022	1.1025	1.1013
3.750×10^{-4}	1.1191	1.1232	1.1242	1.1247	1.1249	1.1244
5.000×10^{-4}	1.1386	1.1422	1.1430	1.1433	1.1435	1.1443
6.250×10^{-4}	1.1557	1.1588	1.1594	1.1597	1.1599	1.1615
7.500×10^{-4}	1.1710	1.1737	1.1742	1.1745	1.1745	1.1767
1.000×10^{-3}	1.1979	1.1999	1.2002	1.2004	1.2004	1.2031
1.250×10^{-3}	1.2214	1.2228	1.2230	1.2231	1.2231	1.2259
1.500×10^{-3}	1.2424	1.2434	1.2435	1.2436	1.2436	1.2463
1.750×10^{-3}	1.2616	1.2623	1.2623	1.2623	1.2623	1.2648
2.000×10^{-3}	1.2792	1.2797	1.2796	1.2796	1.2796	1.2818
2.500×10^{-3}	1.3109	1.3108	1.3107	1.3106	1.3106	1.3121
3.125×10^{-3}	1.3444	1.3440	1.3437	1.3436	1.3436	1.3441
3.750×10^{-3}	1.3722	1.3715	1.3712	1.3711	1.3711	1.3707
5.000×10^{-3}	1.4139	1.4130	1.3126	1.4124	1.4124	1.4111
6.250×10^{-3}	1.4419	1.4411	1.4407	1.4405	1.4405	1.4388
9.375×10^{-3}	1.4781	1.4776	1.4774	1.4771	1.4771	1.4758
1.250×10^{-2}	1.4916	1.4914	1.4913	1.4911	1.4911	1.4903
6.250×10^{-2}	1.4999	1.4999	1.4999	1.4999	1.4999	1.4999

the transform of temperature $\bar{\Theta}_i(Z,\tau)$ subjected to the transformed initial and inlet conditions:

$$\bar{\Theta}_i(Z,0)=0 \quad Z>0 \tag{23a}$$

$$\bar{\Theta}_i(0,\tau)=\bar{f}_i \quad \tau>0 \tag{23b}$$

where

$$\bar{f}_i=\int_0^1 \frac{\Gamma(\lambda_i,R)}{M_i^{1/2}}\,dR. \tag{23c}$$

The infinite system (22) is now solved by finite-differences after truncating with a sufficiently large-order N. Using a second-order accurate explicit finite-difference based on an extension of the Warming and Beam [23] upwind scheme, system (22) becomes:

Predictor:

$$\overline{\bar{\Theta}_{i,j}^{n+1}}=\bar{\Theta}_{i,j}^{n}-Pe\,\zeta\sum_{k=1}^{N}g_{ijk}(\bar{\Theta}_{k,j}^{n}-\bar{\Theta}_{k,j-1}^{n})-Pe\,\Delta\tau\sum_{k=1}^{N}h_{ijk}\bar{\Theta}_{k,j}^{n} \tag{24a}$$

Corrector:

$$\bar{\Theta}_{i,j}^{n+1}=\frac{1}{2}\left[\bar{\Theta}_{i,j}^{n}+\overline{\bar{\Theta}_{i,j}^{n+1}}-Pe\,\zeta\sum_{k=1}^{N}g_{ijk}(\overline{\bar{\Theta}_{k,j}^{n+1}}-\overline{\Theta_{k,j-1}^{n+1}})-Pe\,\zeta\sum_{k=1}^{N}g_{ijk}(\bar{\Theta}_{k,j}^{n}-2\bar{\Theta}_{k,j-1}^{n}+\bar{\Theta}_{k,j-2}^{n})-Pe\,\Delta\tau\sum_{k=1}^{N}h_{ijk}\overline{\bar{\Theta}_{k,j}^{n+1}}\right] \tag{24b}$$

where

$$\zeta=\frac{\Delta\tau}{\Delta Z} \quad \text{and} \quad \bar{\Theta}_{i,j}^{n}\equiv\bar{\Theta}(n\Delta\tau,j\Delta Z) \tag{24c,d}$$

and the superscript $\overline{n+1}$ denotes evaluation at an intermediate time between n and $n+1$.

This system is solved by marching along Z and t up to a final time and axial position and obtaining the transform of temperature $\bar{\Theta}_i(Z,\tau)$. Once the transform $\bar{\Theta}_i(Z,\tau)$ is available, the temperature $\Theta(R,Z,\tau)$ is determined by utilizing the inversion formula (20a).

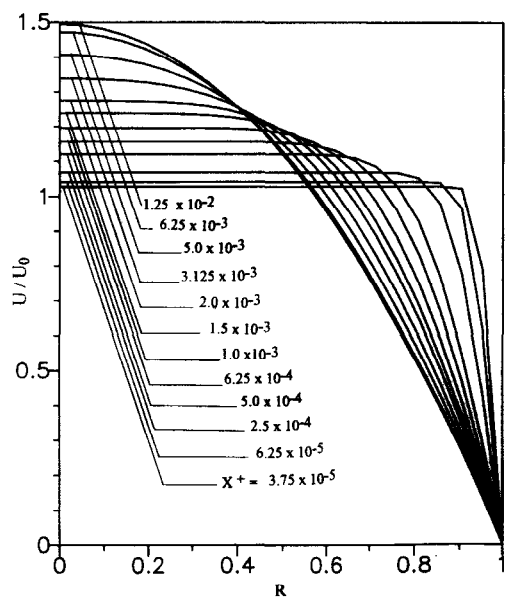

FIG. 1. Velocity profile at different cross sections of the flat duct.

The stability analysis of this finite difference scheme, presented in the appendix, leads to the following stability criterion:

$$0 \leqslant \gamma_i \leqslant 2, \quad i = 1, 2, \ldots, N \tag{24e}$$

where $\gamma_i = C_i \Delta T / \Delta Z$ is the Courant number.

Knowing the dimensionless temperature $\Theta(R, Z, \tau)$, the fluid bulk temperature $\Theta_{av}(Z, \tau)$ can be evaluated from its definition:

$$\Theta_{av}(Z, \tau) = \frac{1}{U_m(Z)} \int_0^1 U(R, Z)\Theta(R, Z, \tau)\, dR \tag{25a}$$

where

$$U_m(Z) = \int_0^1 U(R, Z)\, dR \tag{25b}$$

is the average longitudinal velocity:

Also of interest is the local Nusselt number defined as

$$Nu(Z, \tau) = \frac{4\partial\Theta(1, Z, \tau)/\partial R}{\Theta(1, Z, \tau) - \Theta_{av}(Z, \tau)} = \frac{-4\partial\Theta(1, Z, \tau)/\partial R}{\Theta_{av}(Z, \tau)} \tag{26}$$

since $\Theta(1, Z, \tau) = 0$. However, for computational purposes, it is more convenient to express Θ in terms of its transform, according to the inversion formula (20a), to obtain

$$Nu(Z, \tau) = \frac{-4}{\Theta_{av}(Z)} \sum_{i=1}^{N} \frac{\partial\Gamma(\lambda_i, 1)/\partial R}{M_i^{1/2}} \bar{\Theta}_i(Z, \tau). \tag{27}$$

Since the transform is available from the solution of the system (24), the local Nusselt number is readily evaluated from equation (27).

5. RESULTS AND DISCUSSION

We now present numerical results for the fluid bulk temperature and Nusselt number at different times along the channel. In order to allow comparisons with results available in the literature, the dimensionless axial coordinate is taken as $X^+ = \alpha z / u_0 D_h^2$. We consider two values for the Prandtl number, $Pr = 0.72$ and $Pr = 10$, and the solution of the systems (16a) and (22a) is obtained with $N \leqslant 50$ to observe the convergence behavior.

In the numerical solution of system (22a), the largest eigenvalue of the coefficient matrix was observed to vary slightly with time and position. As the difference is after the fourth decimal place, its effect on the Courant number is negligible. For computations, the Courant number was maintained as 0.93, which greatly reduced the dispersive errors associated with second-order accurate finite-differences schemes. These small oscillations right after the discontinuity are not represented in the figures, since they are by no means relevant to the conclusions that follow.

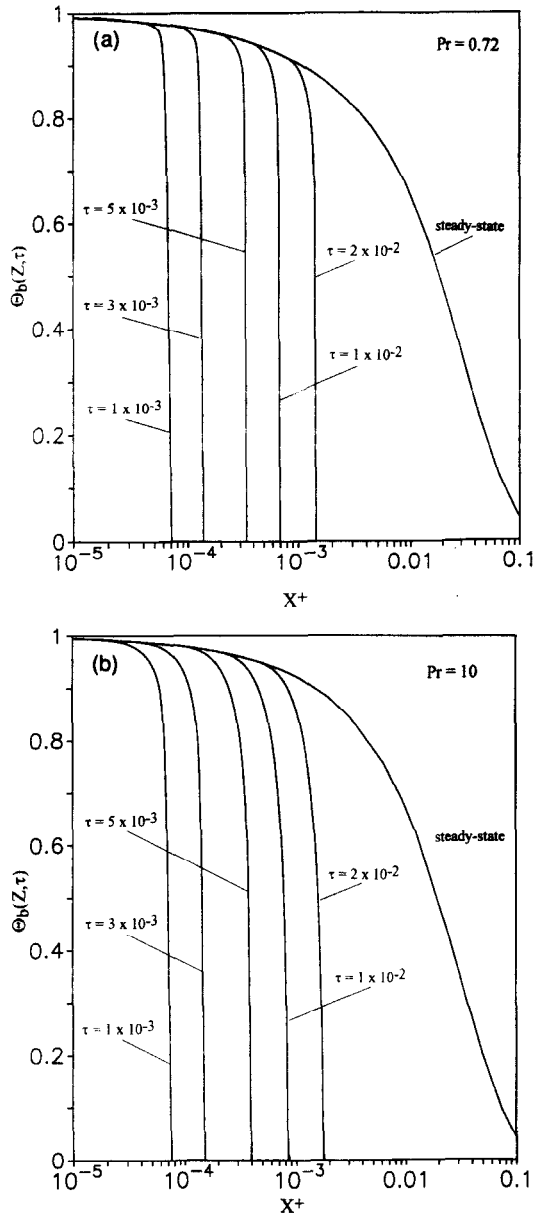

FIG. 2. Fluid bulk temperature at different times for developing flow inside a parallel-plate channel for (a) $Pr = 0.72$, (b) $Pr = 10$.

Table 1 illustrates the convergence behaviour of the dimensionless axial velocity at the duct centerline for different truncation orders N. Clearly, convergence is achieved with a reasonably small number of terms in the series expansion, and requires an increasing N as X^+ decreases. Such results provide accurate predictions when compared with the purely numerical results presented by Shah and Bhatti [2]. The variations of the velocity profile at different cross sections of the flat duct are shown in Fig. 1. For the temperature field, convergence is achieved with four significant digits for $X^+ \geqslant 10^{-3}$ with $N \leqslant 40$. As X^+ is decreased, an increasing number of terms is again required.

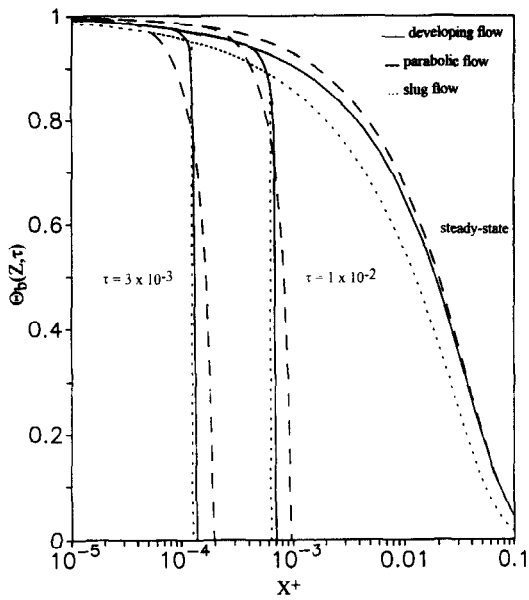

FIG. 3. Comparison of the fluid bulk temperature at different times for slug flow, simultaneously developing flow and parabolic flow.

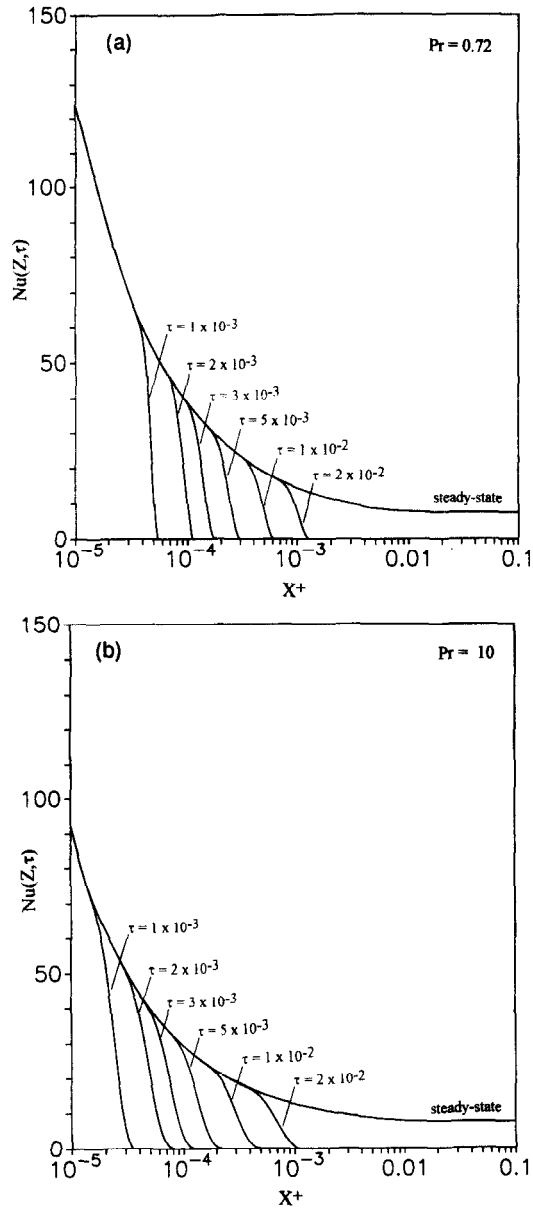

FIG. 4. Local Nusselt number distribution at different times for (a) $Pr = 0.72$, (b) $Pr = 10$.

For slug flow, it is well known that the fluid bulk temperature distribution is divided in two distinct regions, separated by a sharp wave front: (1) a thermally unaffected region, defined by $X^+ > U\tau$, where the fluid has not been disturbed by the thermal wave front and therefore obeys the initial condition; (2) a thermally affected region, defined by $X^+ < U\tau$, where the fluid has already been disturbed by the thermal wave front and therefore obeys the inlet condition imposed by the step jump. However, for a non-slug flow, these two extreme regions are separated by an intermediate region that branches out of the curve for steady-state, as the front advances [24]. In this intermediate region, the faster fluid that obeys the inlet condition interacts with the slower fluid close to the walls, which still obeys the initial condition. These three regions can be identified in Figs. 2(a) and 2(b), which show the fluid bulk temperature plotted as a function of the axial coordinate X^+ at different times τ for $Pr = 0.72$ and $Pr = 10$, respectively.

Figure 3 shows a comparison of the fluid bulk temperature distribution as a function of time for slug flow, simultaneously developing flow and parabolic flow. It is seen that the transient behavior of the developing flow situation is encapsulated by the other two types of flow and the intermediate region is more pronounced for parabolic flow.

Figures 4(a) and 4(b) show the local Nusselt number distribution as a function of axial distance and time for $Pr = 0.72$ and $Pr = 10$, respectively. The local Nusselt number decreases as the Prandtl number increases, as expected, since the slug flow situation ($Pr \to 0$) is the upper limit for the Nusselt number distribution in simultaneously developing flow, whereas the fully developed flow situation ($Pr \to \infty$) is the lower limit. As far as the propagation of the thermal wave is concerned, it is seen that the thermal front in simultaneously developing flow advances slower for increasing Pr, and the observations discussed previously for the fluid bulk temperature can be repeated, except that the thermal wave front indicates that the intermediate region extends farther downstream, although not as pronounced as for the case of fully developed flow [24].

Acknowledgement—One of the authors, R. O. C. Guedes, wishes to acknowledge the financial support provided by CNPq from Brazil.

REFERENCES

1. R. K. Shah and A. L. London, Laminar forced convection in ducts. In *Advances in Heat Transfer* (Edited

by T. F. Irvine and J. P. Hartnett), Suppl. 1. Academic Press, New York (1978).
2. R. K. Shah and M. S. Bhatti, Laminar convective heat transfer in ducts. In *Handbook of Single-Phase Convective Heat Transfer* (Edited by S. Kakac, R. K. Shah and W. Aung), pp. 3.1–3.137. Wiley, New York (1987).
3. W. M. Kays, Numerical solution for laminar flow heat transfer in circular tubes, *Trans. ASME* **77,** 1265–1274 (1955).
4. S. Kakac and M. R. Ozgu, Analysis of laminar flow forced convection heat transfer in the entrance region of a circular pipe, *Wärme- und Stoffübertragung* **2,** 240–245 (1969).
5. G. J. Hwang and J. P. Sheu, Effect of radial velocity component on laminar forced convection in entrance region of a circular tube, *Int. J. Heat Mass Transfer* **17,** 372–375 (1974).
6. H. L. Langhaar, Steady flow in the transition length of a straight tube, *J. Appl. Mech.* **A9,** 55–58 (1942).
7. E. M. Sparrow, S. H. Lin and T. S. Lundgren, Flow development in the hydrodynamic entrance region of tubes and ducts, *Physics Fluids* **7,** 339–347 (1964).
8. J. B. Campos Silva, R. M. Cotta and J. B. Aparecido, Analytical solutions to simultaneously developing laminar flow inside parallel-plate channels, *Int. J. Heat Mass Transfer* **35,** 887–895 (1992).
9. T. M. B. Carvalho, R. M. Cotta and M. D. Mikhailov, Flow development in entrance region of ducts, *Comm. Num. Meth. Engng* **9,** 503–509 (1993).
10. R. M. Cotta, *Integral Transforms in Computational Heat and Fluid Flow*. CRC Press, Boca Raton, FL (1993).
11. T. V. Nguyen, Low Reynolds number simultaneously developing flows in the entrance region of parallel plates, *Int. J. Heat Mass Transfer* **34,** 1219–1225 (1991).
12. C. L. Hwang and L. T. Fan, Finite differences analysis of forced convection heat transfer in entrance region of a flat rectangular duct, *Appl. Scient. Res.* **13,** 401–422 (1964).
13. W. E. Mercer, W. W. Pearce and J. E. Hitchcock, Laminar forced convection in the entrance region between parallel flat plates, *ASME J. Heat Transfer* **89,** 251–257 (1967).
14. R. Siegel and E. M. Sparrow, Simultaneous development of velocity and temperature distributions in a flat duct with uniform wall heating, *A.I.Ch.E. Jl* **5,** 73–75 (1959).
15. L. S. Han, Simultaneous developments of temperature and velocity profiles in flat ducts, *Proceedings Heat Transfer Conference*, Boulder, CO, Part III, pp. 591–597 (1961).
16. C. H. Li, Exact transient solutions of parallel-current transfer processes, *ASME J. Heat Transfer* **108,** 365–369 (1986).
17. R. Siegel, Heat transfer for laminar flow in ducts with arbitrary time variations in wall temperature, *J. Appl. Mech.* **27,** 241–249 (1960).
18. J. Sucec, Analytical solution for unsteady heat transfer in a pipe, *ASME J. Heat Transfer* **110,** 850–854 (1988).
19. T. F. Lin and J. C. Kuo, Transient conjugated heat transfer in fully developed laminar pipe flows, *Int. J. Heat Mass Transfer* **31,** 1093–1102 (1988).
20. W. M. Yan, Y. L. Tsay and T. F. Lin, Transient conjugated heat transfer in laminar pipe flows, *Int. J. Heat Mass Transfer* **32,** 775–777 (1989).
21. D. J. Schutte, M. M. Rahman and A. Faghri, Transient conjugate heat transfer in a thick-walled pipe with developing laminar flow, *Numer. Heat Transfer, Part A* **21,** 163–186 (1992).
22. IMSL Library, *MATH/LIB*. Houston, Texas (1987).
23. R. F. Warming and R. M. Beam, Upwind second-order difference schemes and applications in aerodynamic flows, *AIAA Jl* **14,** 1241–1249 (1976).
24. R. M. Cotta, M. N. Ozisik and D. S. McRae, Transient heat transfer in channel flow with step change in inlet temperature, *Numer. Heat Transfer* **9,** 619–630 (1986).

APPENDIX

Stability analysis

For the purpose of stability analysis, we consider matrices **G** and **H** constant in equation (22a). This equation, in the matrix form, then becomes

$$\frac{\partial \mathbf{y}(Z,\tau)}{\partial \tau} + \mathbf{G}\frac{\partial \mathbf{y}(Z,\tau)}{\partial Z} + \mathbf{H}\mathbf{y}(Z,\tau) = \mathbf{0} \tag{A1}$$

where

$$\mathbf{y}(Z,\tau) = \{\bar{\Theta}_1(Z,\tau), \bar{\Theta}_2(Z,\tau), \ldots, \bar{\Theta}_N(Z,\tau)\}^{\mathrm{t}}. \tag{A2}$$

Next, we define

$$\mathbf{x} = \mathbf{S}^{-1}\mathbf{y} \tag{A3}$$

where

$$\mathbf{S}^{-1}\mathbf{H}\mathbf{S} = \mathbf{K} \tag{A4}$$

$$\mathbf{S}\mathbf{S}^{1} = \mathbf{I} \tag{A5}$$

and **K** is the diagonal matrix containing the eigenvalues of **H**, and **I** is the identity matrix. Then, replacing **y** by **Sx** in equation (A1) and multiplying by $\mathbf{S}^{-1}$:

$$\mathbf{S}^{-1}\mathbf{S}\frac{\partial \mathbf{x}(Z,\tau)}{\partial \tau} + \mathbf{S}^{-1}\mathbf{G}\mathbf{S}\frac{\partial \mathbf{x}(Z,\tau)}{\partial Z} + \mathbf{S}^{-1}\mathbf{H}\mathbf{S}\mathbf{x}(Z,\tau) = \mathbf{0} \tag{A6}$$

or, after substituting for equations (A4) and (A5),

$$\frac{\partial \mathbf{x}(Z,\tau)}{\partial \tau} + \mathbf{S}^{-1}\mathbf{G}\mathbf{S}\frac{\partial \mathbf{x}(Z,\tau)}{\partial Z} + \mathbf{K}\mathbf{x}(Z,\tau) = \mathbf{0}. \tag{A7}$$

We define

$$\mathbf{Q} = \mathbf{S}^{-1}\mathbf{G}\mathbf{S} \tag{A8}$$

and rewrite equation (A7) as

$$\frac{\partial x_i}{\partial \tau} + \sum_{j=1}^{N} Q_{ij}\frac{\partial x_j}{\partial Z} + k_{ii}x_i = 0, \quad i = 1,2,..,N \tag{A9}$$

where k_{ii} is the ith eigenvalue of **H**.

The following change of variables is then defined:

$$x_i^* = \exp(k_{ii}\tau)x_i \tag{A10}$$

which introduced in equation (A9) yields

$$\frac{\partial x_i^*}{\partial \tau} + \sum_{j=1}^{N} Q_{ij}\exp[-(k_{jj}-k_{ii})\tau]\frac{\partial x_j^*}{\partial Z} = 0. \tag{A11}$$

Finally, we define $Q_{ij}^* = Q_{ij}\exp[-(k_{jj}-k_{ii})\tau]$ and substitute this expression in (A11) to obtain

$$\frac{\partial x_i^*}{\partial \tau} + \sum_{j=1}^{N} Q_{ij}^*\frac{\partial x_j^*}{\partial Z} = 0. \tag{A12}$$

Warming and Beam [23] studied the stability of the upwind scheme applied to a model equation similar to equation (A12). In their analysis, the coefficients matrix **Q** was assumed constant in order to apply linear stability theory. Then, by applying a Von Neumann type stability analysis, they showed that the upwind scheme is stable if and only if

$$0 \leqslant c_i\frac{\Delta\tau}{\Delta Z} \leqslant 2, \quad \text{and} \quad c_i > 0 \quad \text{for} \quad i = 1,2,\ldots,N \tag{A13}$$

where c_i are the eigenvalues of $\mathbf{Q}^*$.

It should be noted, however, that, in the case studied here, matrices **G** and **H** are Z-dependent and matrix $\mathbf{Q}^*$ is τ-dependent and, consequently, the eigenvalues c_i vary with Z and τ as well. Although not directly applicable, we apply here the linear stability analysis and select the largest eigenvalue for the estimation of the Courant number.